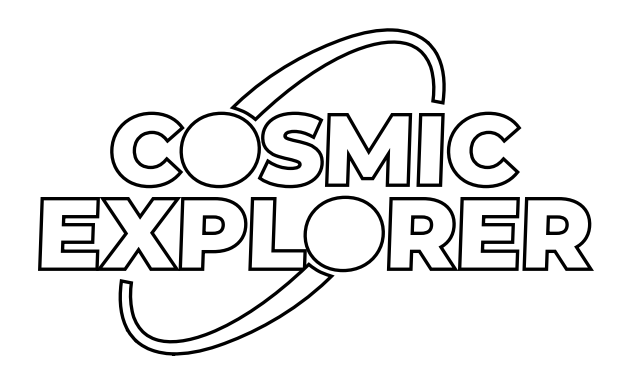
Technical Note CE-T2400017-v1 2024/09/06

Astigmatism considerations for CE recycling/extraction cavity design

Liu Tao^b, Luis Diego Bonavena^a, Sagar Gupta^a, Paul Fulda^a University of Florida, ^bUniversity of California Riverside

This is an internal working note of the COSMIC EXPLORER project.



http://www.cosmicexplorer.org/

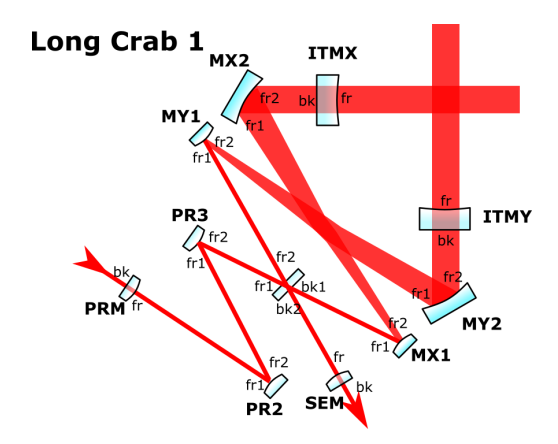


Figure 1: Long Crab1 Layout - A potential layout of the recycling cavities for CE. This layout ensures a small angle and small area of incidence on the Beam-Splitter.

Abstract

The 40km long arms in Cosmic Explorer (CE) necessitate a much larger beam size in the arms compared to LIGO. Therefore, a redesign of the recycling cavities is needed to ensure that the beam shrinks to an appropriate size while also satisfying other conditions, like the beam size at the Beam-Splitter (BS) and the total length of the cavities. To achieve this, various corner interferometer layouts have been proposed [1]. In this document, we cover the theory behind the astigmatism caused by individual optical components in the design and address this problem to create a nearly completely non-astigmatic Power Recycling Cavity (PRC) and a completely non-astigmatic Signal Extraction Cavity (SEC) in a specific realization of the Long Crab1 layout. The method adopted can be extended to other layouts and involves modifying various cavity parameters, such as the Radius of Curvature (RoC) of the mirrors and the beam Angle of Incidence (AoI) on the optics.

Introduction

The following analysis uses a specific configuration for the selection of optical parameters to establish an initial starting point for developing the final configuration of the Cosmic Explorer corner. The parameters listed in (Table 1) are chosen to meet certain design constraints, such as achieving a beam size of approximately 10 mm at the beam splitter ($w_{BS} \sim 10$ mm) and ensuring the SEC length remains below 150 meters ($L_{SEC} < 150$ m). Given that the beam size at the High-Reflection (HR) surface of the Input Test Mass (ITM) is around 100 mm ($w_{HR} = \mathcal{O}(100)$ mm), it needs to be reduced to a few millimeters over a distance of 100-150 meters while maintaining control over the accumulated Gouy phase (see [2]). To achieve this, a highly curved Anti-Reflection (AR) surface of the ITM is proposed, which would initiate the beam shrinking process immediately after transmission out of the arm cavities through the ITMs. As shown in Figure 1, in the Long Crab1 layout there are two mirrors between the ITM and BS namely MX1/MY1 and MX2/MY2 (referred to as M1 and M2 collectively). M1 is a convex mirror (specific to this case) that slows down the converging of the beam so that the beam incident on the beam-splitter is not converging too quickly [3]

Component	Position	Beam Size w	RoC	Acc. Gouy Phase	q
ITM(HR)	0	119.87mm	$30 \mathrm{km}$	0°	24236+11819i
ITM(AR)	$0.2 \mathrm{m}$	119.87 mm	$40 \mathrm{m}$	$186\mu^{\circ}$	-89.165+0.187i
M2	$37.2 \mathrm{m}$	70.13mm	∞	$85.6\mathrm{m}^{\circ}$	-52.165+0.187i
M1	$75.2 \mathrm{m}$	19.044 mm	$40 \mathrm{m}$	$637.7 \mathrm{m}^{\circ}$	-46.111+1.989 <i>i</i>
BS	94.2m	11.2mm	∞	2.36°	-27.111+1.989i

Table 1: Table containing relevant parameters at the optical components in the SEC that are responsible for astigmatism under ideal circumstances.

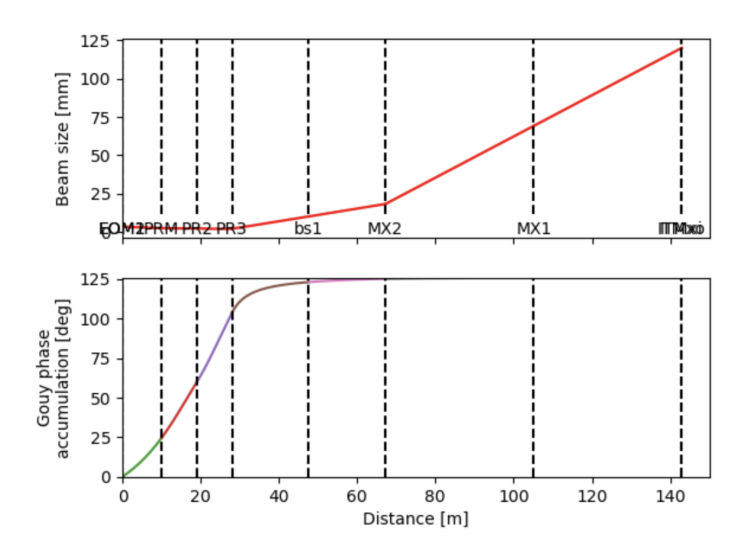


Figure 2: Beam trace of the Power Recycling Cavity of proposed Long Crab 1 model for CE.

and also to allow some accumulation of Gouy phase in the SEC. M2 is nominally a flat mirror and has a large AoI to make sure that beams in X and Y arms remain perpendicular while achieving a small AoI on the beam-splitter and M1. This means that AoI on M2 depends on the AoI on BS as well as M1. In addition to this, to avoid the recombination of possible ghost beams, the ITM is supposed to have a vertical wedge [4]. All these factors indicate that the astigmatism needs to be kept in check to properly mode match the SEC to the ARM cavities. An astigmatic beam at the Signal Extraction Mirror (SEM) can also lead to squeezing losses and misrotation [5, 6].

1 Theoretical description of simple astigmatism in Gaussian beams due to spherical optics

To start, we try to develop a theoretical understanding of how each component in the cavity impacts the overall mode-mismatch. Let us first look at a simple case where a non-astigmatic Gaussian Beam, represented by the parameter q_i , is incident on a curved mirror at an angle. The ABCD matrices are different for both the tangential (x) and sagittal (y) planes and are shown in Eq. (1) and (2) [7].

$$M_x = \begin{pmatrix} 1 & 0\\ \frac{-2n_1}{R_c \cos \alpha_1} & 1 \end{pmatrix} \tag{1}$$

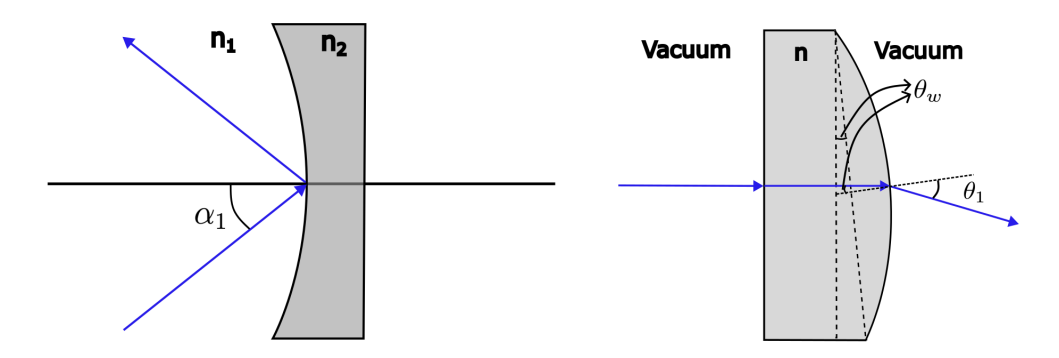


Figure 3: Left- Depiction of a beam reflection off a mirror at an angle α_1 ; Right- Depiction of the ITM lens and the path the beam will take from the ARM cavity into the Recycling Cavities.

$$M_y = \begin{pmatrix} 1 & 0\\ \frac{-2n_1\cos\alpha_1}{R_c} & 1 \end{pmatrix} \tag{2}$$

Where α_1 is the AoI on the mirror, R_c is the radius of curvature and n_1 is the refractive index. Therefore, the reflected beam parameters in the x and y directions are given by

$$q_x = \frac{q_i}{1 - 2q_i n_1 / R_c \cos \alpha_1}$$

$$q_y = \frac{q_i}{1 - 2q_i n_1 \cos \alpha_1 / R_c}$$

From the last two equations we can calculate the Mode-Mismatch (Eq.(3)) ([7]) between the two beam parameters denoted by K, with an approximation that either the AoI or the power of the mirror are very small and hence $q_x \approx q_y$:

$$K = \frac{(q_x - q_y)^*}{(q_x - q_y^*)} \approx \frac{i(q_x - q_y)^*}{2\mathcal{I}\{q_y\}}$$
 (3)

On substituting in the expressions for q_x and q_y , and and applying the small angle approximation, we obtain:

$$|K| \approx \frac{(z^2 + z_R^2)^2 n_1 \alpha_1^2}{z_R R_c} = \left(\frac{w^2 z_R^2}{w_0^2}\right) \frac{n_1 \alpha_1^2}{z_R R_c} = \frac{\pi}{\lambda} \left(\frac{w^2 n_1 \alpha_1^2}{R_c}\right)$$
(4)

where w is the beam size at the mirror, w_0 is the incident beam waist size and λ is the wavelength of light. The derivation for this expression can be found in Appendix A.

In case of a mirror with large angle of incidence and small curvature such as M2 (as seen in Table 1), we can obtain an approximate equation for Mode-Mismatch in a similar way, and the equation is given by:

$$|K| \approx \frac{\pi}{\lambda} \left(\frac{w^2 n_1 \sin^2(\alpha)}{R_c \cos(\alpha)} \right)$$
 (5)

The ABCD matrices in the tangential and sagittal plane for the ITM lens differ slightly compared to that of a mirror. The two matrices are given below

$$M_t = \begin{pmatrix} \cos\theta_1/\cos\theta_w & 0\\ \frac{-\Delta n_t}{R_{ar}} & \cos\theta_w/\cos\theta_1 \end{pmatrix}$$
 (6)

$$M_s = \begin{pmatrix} 1 & 0 \\ \frac{-\Delta n_s}{R_{ar}} & 1 \end{pmatrix} \tag{7}$$

where θ_1 is the AoI at the AR surface, and θ_w is the wedge angle (depicted in Figure 3). The Δn 's are given by

$$\Delta n_t = \frac{n\cos\theta_w - \cos\theta_1}{\cos\theta_w \cos\theta_1}$$
$$\Delta n_s = n\cos\theta_w - \cos\theta_1$$

We also note that the equivalence from the tangential and sagital notation to Cartesian notation is flipped because the wedge is vertical in nature. Following this, the expression for the astigmatism caused by the wedge in the ITM lens under the small angle approximation is very similar to the expression for mirrors and is given by:

$$|K| \approx n^2 (n-1) \frac{\pi}{2\lambda} \frac{w^2}{R_{ar}} \theta_w^2 \left| 1 + \frac{(1+n)}{n^2} \frac{R_{ar}}{q_i} \right|$$

where R_{ar} is the RoC of the AR side of ITM. The additional factor that depends on q_i and R_{ar} can be problematic, however, in our specific case (Table 1), $R_{ar} = \mathcal{O}(10)$ m and $q_i = \mathcal{O}(10000)$ m. Therefore:

$$\left| 1 + \frac{(1+n)}{n^2} \frac{R_{ar}}{q_i} \right| \approx 1 \Rightarrow \left| |K| \approx n^2 (n-1) \frac{\pi}{2\lambda} \frac{w^2}{R_{ar}} \theta^2 \right|$$
 (8)

The astigmatism contributions from the ITM (converging) and M1 (diverging) add up due to their respective natures, therefore M2 is required to be curved in order to cancel/mitigate the astigmatism. The Mode-Mismatch is a complex quantity and has a phase. Therefore, the individual Mode-Mismatch amplitudes do not just simply add or subtract. The phasor diagram in Fig 4 depicts this vector addition and shows how the astigmatism contribution can potentially be cancelled out by controlling the AoI on M1 and RoC of M2 and in turn controlling the mode-mismatch amplitudes. We further explore this strategy, originally proposed in [8], in §2. We would like to note that the strategy in [8] does work on the assumption that astigmatisms either add or subtract, though. Hence they always have some residual mismatch due to the phase mismatch.

2 Astigmatism free SEC design for CE

Following Fig 4, we can mathematically express the total astigmatic mode-mismatch as

$$K = |K_{ITM}| + |K_{M1}|e^{i\phi_1} - |K_{M2}|e^{i\phi_2}$$

$$\Rightarrow |K|^2 = (|K_{M1}|\cos(\phi_1) + |K_{ITM}| - |K_{M2}|\cos(\phi_2))^2 + (|K_{M1}|\sin(\phi_1) - |K_{M2}|\sin(\phi_2))^2$$
(9)

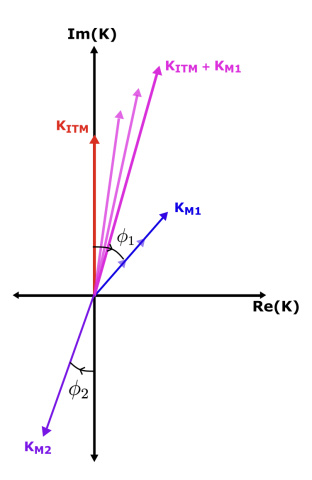


Figure 4: Phasor diagram of the different contributions in the Long Crab 1 layout. Each arrow represents the Mode-Mismatch K introduced by each optical element in the model. The imaginary part is two times the Gouy phase accumulated between two consecutive optical elements.

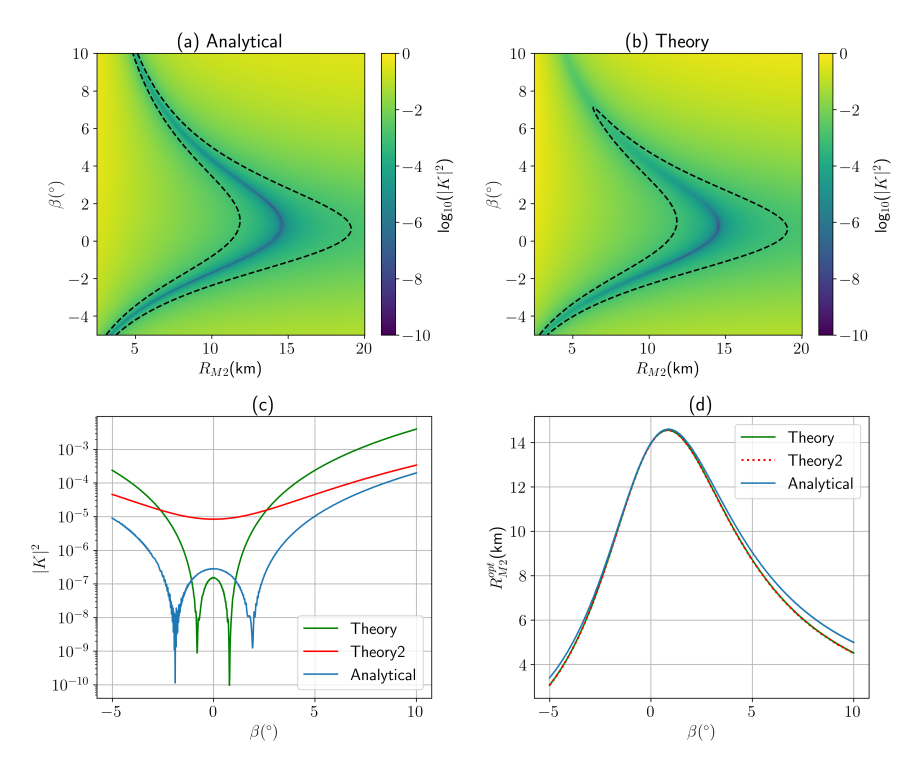


Figure 5: (a), (b): Heat maps of power Mode Mismatch ($|K|^2$) as a function of AoI on M1(β) and RoC of M2 (R_{M2}) given by Analytical and Theoretical models respectively. $|K|^2 < 10^{-3}$ in the region enclosed by the contours; (c) Minimum mode mismatches possible for a given β ; (d) R_{M2} that minimizes $|K|^2$ (R_{M2}^{opt}).

Upon substituting in the expressions of mode mismatch for individual components and minimising $|K|^2$ for a given AoI β on M1 by taking the derivative with respect to R_{M2} , we obtain the following expression for R_{M2}^{opt}

$$\frac{1}{R_{M2}^{opt}} = \left(\frac{w_{M1}^2}{R_{M1}}\beta^2 \cos(\phi_1 - \phi_2) + n^2 \Delta n \frac{w_{ar}^2}{2R_{ar}}\theta_w^2 \cos(\phi_2)\right) / \left(w_{M2}^2 \frac{\sin^2(\gamma)}{\cos(\gamma)}\right)$$
(10)

where w's and R's are the waist sizes and RoCs on respective components and γ is the AoI on M2, and R_{M2}^{opt} is the value of R_{M2} that minimizes Mode-Mismatch for a given β . γ depends on β to keep the X and Y arms perpendicular to each other given by:

$$\gamma = \frac{\pi/4 + 2\beta - \theta_{BS}}{2} \tag{11}$$

where θ_{BS} is the AoI on the Beam-Splitter.

Now, let us consider the phases of the Mode-Mismatches. Intuitively, it makes sense that the phases ϕ_1 and ϕ_2 are twice the accumulated Gouy phase between the ITM and M1 and M2 respectively, since mode mismatch due to astigmatism leads to scattering of the fundamental mode into second order modes. But the mathematical expressions tell us that it is not quite the case. If we trace the derivation for Mode-Mismatch(A), we find that $K \propto q_f^2$ where q_f is the beam parameter after the reflection or refraction off of the particular component. This suggests that the phases are actually twice the difference between the local Gouy phases of the final beams. In case of ϕ_2 , the accumulated Gouy phase and the local phase difference are the same since M2 is supposed to be weakly curved, but for ϕ_1 the two quantities differ (albeit both being close to zero since the accumulated Gouy phase is very small and the beam size at M1 is still significantly larger than the waist size). Since they are not so different, and have a small effect on the value of R_{M2}^{opt} as evident from Eq. 10 with w_{M1} smaller than w_{ar} by a factor of 6 (Fig 2 and Table 1). While R_{M1} and R_{ar} are comparable in magnitude, both approaches should give a very similar dependence of R_{M2}^{opt} on β , but we should see a significant difference in minimum total mode-mismatch possible.

Figure 5 shows the heat map of Mode-Mismatch between the q_x and q_y direction when we sweep the R_{M2} vs β parameter space for the *Theoretical* and *Analytical* models. The Theoretical model uses the mode mismatch expression given by 9, and the Analytical model uses the ABCD matrices to propagate the beam from the ITM lens all the way to the BS and calculates the exact mode-mismatches. It is important to note that the only approximation we make in the *Theoretical* model is the small angle approximation along with the assumption that the complex Mode-Mismatches due to the three components simply add up, while there are no approximations made for the Analytical model. The Theory2 curves in Figure 5 (c) and (d) correspond to the phase terms in Eq. 9 being twice the accumulated gouy phases instead of twice the difference in local gouy phases. We clearly see that R_{M2}^{opt} is mostly identical in both cases. However, the minimum possible mode-mismatches are very different. There is still some deviation between the *Theory* and *Analytical*. This can be explained by the assumption that the beam incident on the individual components is non-astigmatic and becomes astigmatic after reflection/refraction, which is not exactly the case for MX1 and MX2. As expected both curves follow the Analytical curve closely around $\beta = 0$. It is also important to note that the heat map is not symmetric around $\beta = 0$. This is a result

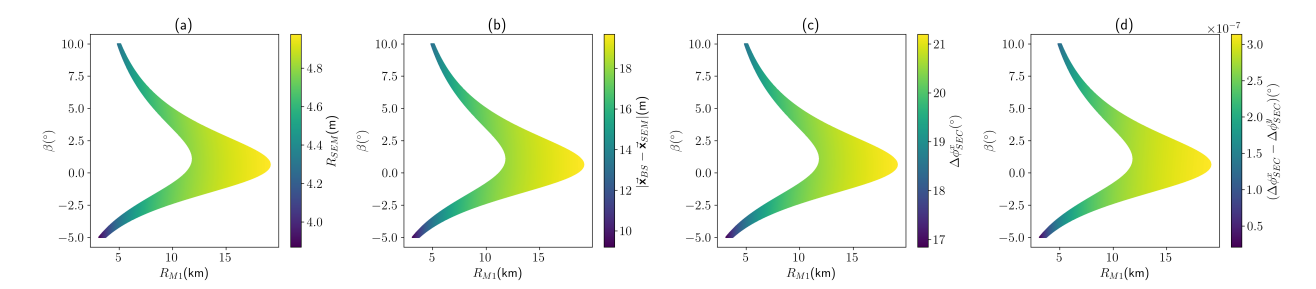


Figure 6: Variation of different parameters in the SEC in $|K|^2 < 10^{-3}$ region. (a) RoC of the SEM; (b)Distance of SEM from the BS (while keeping the beam size at SEM at 2mm); (c) Total one way gouy-phase accumulation in the SEC in the x-direction; (d) Difference in gouy-phase accumulation in the x and y direction

of dependence of AoI on M2 (γ) on β in Eq. (11). All of this indicates that we have a solid understanding of how to mitigate astigmatism in this specific arrangement of optical components.

Now that we know we have a solution to our problem, it is important to know how viable these solutions are. There are several concerns that we need to address before we make a conclusion. The first one is the variation in the beam parameter at the BS and consequently at the SEM. This also necessitates a change in the RoC of the SEM to keep the cavity modematched to the ARMs. We also want to make sure that we are accumulating enough Gouy phase in the SEC which might change as well. To combat this we need to adjust the distance between the SEM and the BS, while making sure that beam-size is not too small at the SEM (>2mm). In Figure 6 (a) - (c) we show how all these parameters change in the $|K|^2 < 10^{-3}$ region. We see that R_{SEM} , $|\vec{\mathbf{x}}_{BS} - \vec{\mathbf{x}}_{SEM}|$ as well as the total one way accumulated Gouy phase in the SEC ($\Delta \phi_{SEC}$) do not change much in the $0^{\circ} < \beta < 2^{\circ}$ region. There is also the concern of accumulated Gouy phase differing significantly in the x and y directions, which could lead to issues in alignment and sensing control of the components. This is addressed in Figure 6 (d) which tells us that this difference is extremely small. The beam is astigmatic only between the ITM and the M1 mirrors if we try to minimize astigmatism everywhere else. Since the accumulated Gouy phase between ITM an M1 is very small to begin with ($\sim 0.7^{\circ}$), the difference in the two directions will be extremely small. Therefore, the tolerances on the various RoCs and AoIs seem to be manageable at the first glance.

3 Astigmatism free PRC design for CE

Now that we have shown that the SEC can be made astigmatism free, let us turn our attention to the Power Recycling Cavity (PRC). The two mirrors that contribute to the astigmatism in addition to those discussed for the SEC are PR2 and PR3 as shown in Figure 1. A simple method for astigmatic compensation for a folded resonator like the PRC and applicable to the PR2 and PR3 mirrors is discussed by Qiao et.al.([9]). If we look at the beam approaching from BS to PR3, it becomes astigmatic after reflection. If we have a waist occurring between PR3 and PR2, the beam sizes in the two directions should become equal once again after the waist. If PR2 is placed at this intersection with the correct RoC and AoI the beam reflected

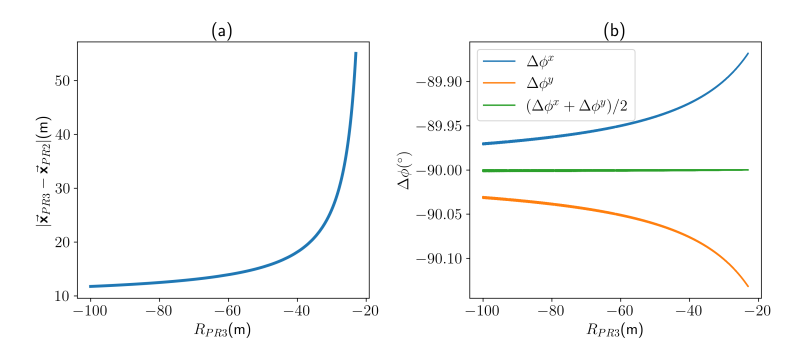


Figure 7: (a) Distance of PR2 from PR3 as a function of RoC of PR3 for a fixed AoI on PR3 required to cancel out the astigmatism, (b) Accumulated one way Gouy Phase between PR2 and PR3.

off of PR2 will astigmatism free. However, the requirement of a waist seems to be a problem, as that would mean that the accumulated Gouy phase between PR2 and PR3 is larger than 45° , which is required for the actuation control of the mirrors. Figure 7 shows that if PR2 is placed at the intersection point, while varying R_{PR3} , the accumulated Gouy phase is always around 90° . This seems to be requirement for the intersection to happen in the first place and can be verified for different layouts and beam sizes. Therefore, it seems impossible to make the PRC completely astigmatism free, but it can still be minimized by reducing the AoIs on PR2 and PR3 as has been done for aLIGO. One can still try to minimize the astigmatism if the accumulated Gouy phase is somewhat close to 90° . We will study that in greater detail in a future technical note.

4 Conclusion and Future Work

In this document, we have studied the contribution of each mirror that introduces astigmatism to the total Mode-Mismatch of the Signal Extraction and Power Recycling Cavities, in the context of the Modified Long Crab 1 layout. We approach the problem by propagating the beam from ITM to the beam splitter and studying the individual contributions using a Mode-Mismatch heat map. We also try to understand these contributions using two different models - Intuitive and Analytical, and find the two models largely agree with each other and with the simulations in the small β regime. In doing so, we have successfully shown that the SEC in CE can be made completely astigmatic while using only spherical optics. We also study the astigmatism in the PRC, where PR2 and PR3 are the additional mirrors that need to be accounted for. It is possible to completely cancel out the contributions from the two mirrors with a strict requirement that the one way accumulated Gouy phase between the two mirrors is 90°, which is at odds with the 45° requirement for the actuation of the mirrors. Regardless, since the incident beam sizes on the two mirrors are small, their contributions can largely be minimised just by reducing the AoIs.

In further studies, we aim to study the effect a closed cavity might have on the modemismatch. We also need to study the tolerances on all the optics and if these tolerances can be controlled with thermal compensation and actuation in greater depth. There are other effects such as aberrations and the Mode-Healing/Harming effect of the cavities that might play a very important role in narrowing the set of parameters. We will also like to extend this to study the possibility of a similar design in the Y-arm with Schnupp Asymmetry perfectly mode-matched to the X-arm with similar parameters.

A Single Pass Mode-Mismatch expression

Starting off with the expression for Mode-Mismatch in Eq (3), we want to obtain the expressions for q_x and q_y . Evaluating the expression for q_y , we get

$$q_{y} = \frac{q_{i}}{1 - 2q_{i}n_{1}\cos\alpha_{1}/R_{c}} \Rightarrow q_{y} = \frac{z + iz_{R}}{(1 - \frac{2n_{1}z\cos\alpha_{1}}{R_{c}}) - i\frac{2n_{1}z_{R}\cos\alpha_{1}}{R_{c}}}$$

$$\Rightarrow q_{y} = \frac{z - \frac{2n_{1}\cos\alpha_{1}}{R_{c}}(z^{2} + z_{R}^{2})}{(1 - \frac{2n_{1}z\cos\alpha_{1}}{R_{c}})^{2} + (\frac{2n_{1}z_{R}\cos\alpha_{1}}{R_{c}})^{2}} + i\frac{z_{R}}{(1 - \frac{2n_{1}z\cos\alpha_{1}}{R_{c}})^{2} + (\frac{2n_{1}z_{R}\cos\alpha_{1}}{R_{c}})^{2}}$$

$$\Rightarrow \mathcal{I}\{q_{y}\} = \frac{z_{R}}{(1 - \frac{2n_{1}z\cos\alpha_{1}}{R_{c}})^{2} + (\frac{2n_{1}z_{R}\cos\alpha_{1}}{R_{c}})^{2}}$$

We can also evaluate the numerator in terms of the input beam parameter

$$q_{x} - q_{y} = \frac{q_{i}}{1 - 2q_{i}n_{1}/R_{c}\cos\alpha_{1}} - \frac{q_{i}}{1 - 2q_{i}n_{1}\cos\alpha_{1}/R_{c}}$$

$$\Rightarrow q_{x} - q_{y} = \frac{q_{i}(1 - 2q_{i}n_{1}\cos\alpha_{1}/R_{c}) - q_{i}(1 - 2q_{i}n_{1}/R_{c}\cos\alpha_{1})}{1 + \frac{4n_{1}^{2}q_{i}^{2}}{R_{c}^{2}} - \frac{2n_{1}q_{i}}{R_{c}}(\cos\alpha_{1} + \sec\alpha_{1})}$$

$$\Rightarrow \left[q_{x} - q_{y} = \left(\frac{2q_{i}^{2}n_{1}}{R_{c}}\right)\left(\frac{\sin^{2}\alpha_{1}}{\cos\alpha_{1}}\right) / \left(1 + \frac{4n_{1}^{2}q_{i}^{2}}{R_{c}^{2}} - \frac{2n_{1}q_{i}}{R_{c}}(\cos\alpha_{1} + \sec\alpha_{1})\right)\right]$$

Plugging these two expressions back into the expression for the amplitude mode-mismatch and taking the modulus on both sides, we get

$$|K_{M1}| = \left(\frac{|q_i|^2 n_1}{z_R R_c}\right) \left(\frac{\sin^2 \alpha_1}{\cos \alpha_1}\right) \cdot \left\{\frac{\left(1 - \frac{2n_1 z \cos \alpha_1}{R_c}\right)^2 + \left(\frac{2n_1 z_R \cos \alpha_1}{R_c}\right)^2}{\left|\left(1 + \frac{4n_1^2 q_i^2}{R_c^2} - \frac{2n_1 q_i}{R_c}(\cos \alpha_1 + \sec \alpha_1)\right)\right|}\right\}$$
(12)

Under small angle approximation, we get:

$$|K_{M1}| \approx \frac{|q_i|^2 n_1 \alpha_1^2}{z_R R_c}$$
 (13)

Now we plug in $q_i = z + iz_R$, to get:

$$|K_{M1}| \approx \frac{(z^2 + z_R^2)^2 n_1 \alpha_1^2}{z_R R_c} = \left(\frac{w^2 z_R^2}{w_0^2}\right) \frac{n_1 \alpha_1^2}{z_R R_c} = \frac{\pi}{\lambda} \left(\frac{w^2 n_1 \alpha_1^2}{R_c}\right)$$

In case of a mirror like M2 with a large AoI, but also with a very large RoC, we can still make the following approximation

$$\frac{\left(1 - \frac{2n_1z\cos\alpha_1}{R_c}\right)^2 + \left(\frac{2n_1z_R\cos\alpha_1}{R_c}\right)^2}{\left|\left(1 + \frac{4n_1^2q_i^2}{R_c^2} - \frac{2n_1q_i}{R_c}(\cos\alpha_1 + \sec\alpha_1)\right)\right|} \approx 1$$
(14)

since $R_c >> |q_i|$, which leads to:

$$|K_{M2}| \approx \frac{\pi}{\lambda} \left(\frac{w^2 n_1}{R_c}\right) \left(\frac{\sin^2 \alpha_1}{\cos \alpha_1}\right)$$
 (15)

The expression for K_{ITM} can be derived in a similar way.

References

- [1] Paul Fulda. Cosmic explorer corner layouts: design considerations and down selection. Technical report, Cosmic Explorer DCC. Available at https://dcc.cosmicexplorer.org/CE-T2400012.
- [2] TBD. Draft design of the cosmic explorer signal extraction cavity. Technical report, Cosmic Explorer DCC. Available at TBD.
- [3] Matthew Todd and Stefan W. Ballmer. Beamsplitter in a strongly convergent telescope. Technical report, Cosmic Explorer DCC. Available at https://dcc.cosmicexplorer.org/CE-T2300014.
- [4] Sagar Gupta, GariLynn Billingsley, Jonathan Richardson, and Stefan Ballmer. Considerations for a strong ITM lens in the Cosmic Explorer optical design. Technical report, Cosmic Explorer DCC. Available at TBD.
- [5] Kevin Kuns and Daniel D. Brown. Quantum degradations due to mode mismatch and higher order effects in gravitational wave detectors. *In preparation*. https://dcc.cosmicexplorer.org/CE-P2400005.
- [6] L. McCuller et al. LIGO's quantum response to squeezed states. *Phys. Rev. D*, 104(6):062006, 2021.
- [7] A. E. Siegman. Lasers. University Science Books, 1986.
- [8] N. Man P. Hello. *Design of a low-loss off-axis beam expander*. Virgo-Technical Documentation System, Report No. VIR-NOT-LAS-1390-12, 1996.
- [9] Wen Qiao, Zhang Xiaojun, Wang Yonggang, Sun Liqun, and Niu Hanben. A simple method for astigmatic compensation of folded resonator without brewster window. *Optics Express*, 22:2309, JAN 2014.